

Nonlinear Rheology of a Nanoconfined Simple Fluid

Lionel Bureau*

Institut des Nanosciences de Paris, UMR 7588 CNRS-Université Paris 6, 140 rue de Lourmel, 75015 Paris, France

(Received 10 December 2009; published 25 May 2010)

We probe the rheology of the model liquid octamethylcyclotetrasiloxane (OMCTS) confined into molecularly thin films, using a unique surface force apparatus allowing us to explore a large range of shear rates and confinement. We thus show that OMCTS under increasing confinement exhibits the viscosity enhancement and the nonlinear flow properties characteristic of a sheared supercooled liquid approaching its glass transition. Besides, we study the drainage of confined OMCTS via the propagation of “squeeze-out” fronts. The hydrodynamic model proposed by Becker and Mugele [*Phys. Rev. Lett.* **91**, 166104 (2003)] to describe such front dynamics leads to a conclusion in apparent contradiction with the dynamical slowdown evidenced by rheology measurements, which suggests that front propagation is not controlled by large scale flow in the confined films.

DOI: 10.1103/PhysRevLett.104.218302

PACS numbers: 64.70.pm, 83.50.Lh, 83.60.Rs

Supercooled liquids share qualitative rheological features upon approaching the glass transition [1]: (i) their viscosity increases dramatically, and (ii) they exhibit non-newtonian properties (shear thinning) when the time scale of mechanical forcing becomes shorter than that of structural relaxation. The precise origin of such a behavior is the subject of active theoretical and numerical investigations [2]. Recently, an extension to flow situations of the mode-coupling theory has been proposed, in order to describe this nonlinear rheology [3]. Now, a stringent test of theoretical predictions against experimental results requires measurements, over a large range of shear rate ($\dot{\gamma}$), of the nonlinear properties as jamming is gradually approached. These are extremely challenging to perform on atomic glass formers, because of their elevated glass transition temperature and flow stress. The most comprehensive studies to date have focused on colloidal suspensions of thermosensitive particles, in which the volume fraction, hence the distance to jamming, can be finely tuned [4]. It has thus been shown that, in very good agreement with mode-coupling theory, the flow stress of such suspensions exhibits a rate dependence all the weaker that the distance to glass transition is small, until a yield stress develops when the suspension gets jammed [4]. Such a behavior can be considered as the rheological hallmark of the approach to glass transition.

Here, we show that increasing confinement is an alternative pathway to bring a system close to its jammed state under well-controlled conditions. Surface force apparatus (SFA) experiments have shown that simple liquids confined between solid walls below thicknesses of a few molecular diameters exhibit enhanced flow resistance [5]. From SFA experiments probing the linear response of ultrathin liquid films, Demirel and Granick (DG) concluded to a confinement-induced dynamical slowdown, akin to what occurs in supercooled liquids [6]. However, this conclusion has been challenged by other groups probing the large strain shear response of confined fluids [7,8]. Moreover, experiments by Becker and Mugele (BM) have

shown that a confined liquid drains stepwise by expelling monolayers via the propagation of “squeeze-out fronts” [9]. A model of the front dynamics, extending the work of Persson and Tosatti [10], led them to conclude that the confined fluid essentially retained its bulk viscosity.

The nature of the mechanisms by which the properties of liquids are affected by confinement at the molecular scale therefore remains an open question. Such an issue, which is of interest for the fundamental understanding of the jamming transition [11], is also of paramount importance for boundary lubrication [12], and for nanofluidics, where the knowledge of the flow properties of liquids confined into nm-sized channels or structures is crucial [13].

In this Letter, we provide data that reconcile previous seemingly conflicting observations [6,9]. We report on the first SFA study in which *both* large strain shear rheology and squeeze-out front measurements are performed, in the same experimental run, on the nonpolar liquid octamethylcyclotetrasiloxane (OMCTS), which has been used in the aforementioned works. (i) We show unambiguously, from flow curves measured over 6 decades of $\dot{\gamma}$, that OMCTS under increasing confinement exhibits the viscosity enhancement and non-Newtonian features of a supercooled liquid approaching the glass transition. We thus extend to steady flow situations the early work of DG on linear response, and provide an independent confirmation of their conclusions. (ii) We observe squeeze-out front dynamics in quantitative agreement with that previously reported [9]. When analyzed within the framework of the BM model, it results in an effective viscosity 2 orders of magnitude lower than that directly measured in shear. We conclude that such an apparent contradiction arises from an improper assumption by BM about the nature of the mass transport mechanism at play during front propagation.

Experiments were performed on a home-built SFA [14] (Fig. 1). The liquid is confined between two atomically smooth backsilvered mica sheets glued onto crossed cylindrical lenses (radius of curvature ~ 1 cm). The normal

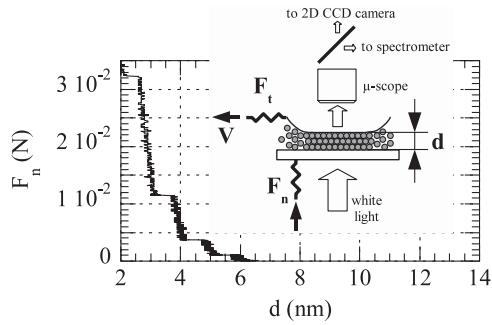


FIG. 1. Force vs distance curve during approach of the surfaces (loading velocity $0.5 \text{ nm}\cdot\text{s}^{-1}$). Inset: scheme of the setup. White light is shone on the confined film, and the transmitted intensity is sent (i) to a spectrometer for spectral analysis [15], and (ii) to a CCD camera acquiring images of the contact area A at a rate of 55 s^{-1} .

force F_n is measured by means of a load cell of stiffness 9500 N m^{-1} . The “contact” area A , over which the mica sheets elastically flatten to form a circular parallel gap in which the liquid is confined, is monitored by videomicroscopy. The thickness of the film, d , is determined by multiple beam interferometry [15] and fast spectral correlation [14,16]. Once confined under a given load, over an area A , the liquid is sheared, in a plane Couette geometry, by moving laterally one surface at a velocity V in the range 10^{-4} – $10^2 \mu\text{m s}^{-1}$, while measuring the resulting tangential force F_t with a cell of stiffness 5200 N m^{-1} . The shear stress sensitivity of the instrument is $F_t/A \sim 200 \text{ Pa}$. Our SFA has the unique feature of using the normal force signal as the input of a feedback loop, which allows us to perform steady-state experiments over large shear amplitudes (up to hundreds of microns) under constant normal load conditions, whatever the level of confinement of the liquid. The mica sheets were prepared as described in [17], glued onto the cylindrical lenses using a UV curing glue (NOA 81, Norland), and cleaved with adhesive tape immediately before being installed in the SFA, so as to obtain contaminant-free surfaces [18]. OMCTS from Fluka (purity grade $\geq 99\%$) was vacuum distilled before use. A drop ($\sim 150 \mu\text{l}$) of the liquid, filtered through a $0.2 \mu\text{m}$ membrane, was injected between the surfaces. It was then left at $T = 20 \pm 0.01 \text{ }^\circ\text{C}$ for 12 h in the sealed SFA, containing P_2O_5 to scavenge residual moisture, before beginning experiments.

Figure 1 shows a force-distance profile measured upon quasistatic approach of the surfaces: it is clearly seen that below 6 nm, the thickness of the confined liquid decreases by steps of approximately 8 \AA , which corresponds to the minor diameter of the slightly oblate OMCTS molecule. This reflects the well-documented wall-induced layered structure of the fluid, which gives rise to the so-called solvation forces [19].

We first focus on shear experiments performed on layered OMCTS films with thicknesses ranging from 6 down to 2 monolayers. Over the whole range of confinement and

velocity explored, we have observed: (i) a smooth stable shear response [see time trace in the inset of Fig. 2(b)], and (ii) a steady-state value of F_t which increases with V . On Fig. 2(a), we plot the steady-state flow stress $\sigma = F_t/A$ versus shear rate $\dot{\gamma} = V/d$ for the different film thicknesses. The same data are plotted on Fig. 2(b) as the effective viscosity $\eta_{\text{eff}} = \sigma/\dot{\gamma}$ versus $\dot{\gamma}$.

It can be seen that, as the OMCTS thickness is reduced from $n = 6$ to 2 monolayers: (i) The flow stress, and hence the viscosity, steadily increases [20]. (ii) The dependence of σ on $\dot{\gamma}$ shifts from linear (Newtonian) to sublinear (shear thinning). (iii) The crossover shear rate, $\dot{\gamma}_c$, above which non-Newtonian behavior is observed, shifts to smaller values. (iv) For $n \leq 4$ monolayers, power-law shear thinning ($\sigma \sim \dot{\gamma}^\alpha$, $\alpha < 1$) at low $\dot{\gamma}$ crosses over to a quasiplateau regime.

The observed viscosity enhancement is in qualitative agreement with previous atomic force microscopy (AFM) measurements on the same liquid [21,22]. A new and key point here is that beyond such a viscosity increase, the full set of rheological features, i.e., the dependence of η_{eff} on $\dot{\gamma}$

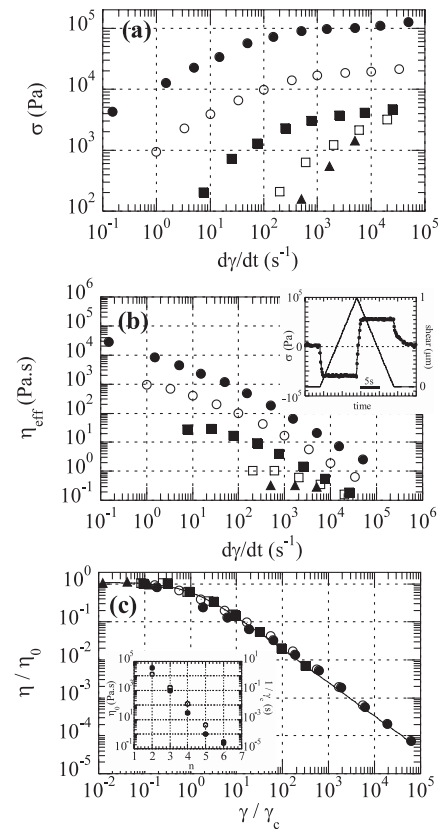


FIG. 2. (a) $\sigma(\dot{\gamma})$ for OMCTS films of (\blacktriangle) 6, (\square) 5, (\blacksquare) 4, (\circ) 3, and (\bullet) 2 monolayers. (b) $\eta_{\text{eff}}(\dot{\gamma})$, symbols as in (a). Inset: time trace of (\bullet , left scale) σ measured at $V = 0.1 \mu\text{m}\cdot\text{s}^{-1}$ on a 2 nm-thick film, (line, right scale) the forth and back shear motion applied. (c) Master curve showing data from (b) plotted as η_{eff}/η_0 vs $\dot{\gamma}/\dot{\gamma}_c$. The solid line is a fit of the form $\eta_{\text{eff}}/\eta_0 = 1/(1 + \dot{\gamma}/\dot{\gamma}_c)^{0.88}$. Inset: values for η_0 (\bullet , left scale) and $1/\dot{\gamma}_c$ (\circ , right scale) used for each n .

and n , is indicative of the approach to jamming [2–4]. This is further supported by the fact that $\eta_{\text{eff}}(\dot{\gamma})$ curves measured for different n collapse onto a single master curve when plotted as η_{eff}/η_0 vs $\dot{\gamma}/\dot{\gamma}_c$, with η_0 the zero shear viscosity [Fig. 2(c)]. Such a collapse, common for bulk liquids sheared at different distances from their glass transition, strongly suggests here that confinement controls the distance to jamming. The inset of Fig. 2(c) shows that both $1/\dot{\gamma}_c$ (i.e., the relaxation time of the liquid) and η_0 sharply increase as the film thickness is decreased. Besides, the reduced viscosity obeys $\eta_{\text{eff}}/\eta_0 \approx 1/(1 + \dot{\gamma}/\dot{\gamma}_c)^{0.88}$, which is consistent with theoretical predictions for sheared supercooled systems [2]. Finally, the observation of a quasiplateau regime which does not extend down to the lowest shear rates indicates that, in the present experiments, confined OMCTS approaches but does not reach jamming. This is consistent with the fact that [see inset of Fig. 2(b)], upon cessation of shear, the stress relaxes (i) very slowly, over ~ 5 s, and (ii) down to a nonmeasurable level.

These observations lead us to conclude, in good agreement with DG [6], that OMCTS undergoes dynamical slowdown upon increasing confinement, similarly to a supercooled system close above jamming. Such a conclusion contrasts with that of Klein [7] or Israelachvili [8], who observed responses exhibiting a stick-slip dynamics which they interpret as shear melting of a confinement-induced ordered solidlike structure. Such a discrepancy might have two origins. (i) The use of different protocols for mica surface preparation: Indeed, the method employed in [7,8], in contrast to that described above, may lead to surface contamination by a submonolayer of nanoparticles, which have been suggested as a possible reason for the observed stick-slip behavior [23]. (ii) Differences in the crystallographic alignment of the confining surfaces, which is expected to affect the shear response of the intercalated molecular film [24]. No systematic investigation have been made so far of the effect of alignment between contaminant-free surfaces, and we therefore cannot discriminate between point (i) and (ii) above to explain differences.

We now present the results from squeeze-out experiments. During loading, we record the light intensity transmitted through the contact area, along with F_n and d . We observe, as in [9,17], that a film of thickness n monolayers drains via nucleation/growth of a circular region of thickness $(n - 1)$ layers (see Fig. 3). Nucleation is accompanied by elastic relaxation of the confining sheets, which are locally bent in the boundary zone connecting the regions of thickness $n - 1$ and n (Fig. 3 inset). This creates a 2D pressure gradient which then drives the monolayer expulsion [9]. The local curvature of the mica sheets induces a contrast in the transmitted intensity [Figs. 3(a)–3(c)] which allows us to follow with time the position of the “squeeze-out” front. We have thus measured, for successive $n \rightarrow n - 1$ transitions, the squeeze-out time τ needed to expel one monolayer from the contact area A . We have done so

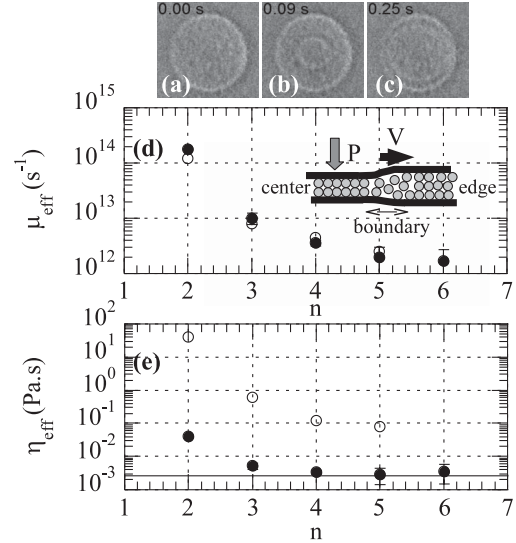


FIG. 3. (a)–(c): Sequence of images ($96 \times 96 \mu\text{m}^2$) showing the front propagation during a $3 \rightarrow 2$ transition. (d): μ_{eff} vs n (number of monolayers). (●) our results, (○) BM results, adapted from [9]. Inset: schematic cross section of the film during squeeze-out. (e): η_{eff} vs n . (○) measured in shear, and (●) deduced from squeeze-out experiments. The horizontal line indicates the bulk viscosity of OMCTS.

before and after rheology experiments, and did not observe any influence of shear history on front dynamics.

In the Persson and Tosatti (PT) model [10], the front velocity is related to the 2D pressure gradient by: $\nabla p_{2D} = -\rho_{2D}\mu_{\text{eff}}V$, where $p_{2D} \sim Pa$ and $\rho_{2D} = \rho a$ [$P = F_n/A$ is the applied pressure, ρ the fluid density and a the molecular size), V is the front velocity and μ_{eff} a viscous drag coefficient. The latter is deduced from the squeeze-out time as [10]: $\mu_{\text{eff}} = 4\pi\tau P/(\rho A)$. On Fig. 3(d) we have plotted μ_{eff} as a function of film thickness for our experiments, along with the values obtained by BM [9]. There is quantitative agreement between both data sets. BM have extended the PT model by assuming that front propagation is controlled by a “layered” Poiseuille flow between the front and the edge of the confinement area (Fig. 3 inset), and thus proposed that μ_{eff} should identify with the drag coefficient of a Hele-Shaw flow, i.e., $\mu_{\text{eff}} = 12\tilde{\eta}_{\text{eff}}/(\rho d^2)$, with $\tilde{\eta}_{\text{eff}}$ a shear viscosity and d the film thickness [9]. We use this expression to infer $\tilde{\eta}_{\text{eff}}(d)$ from the front dynamics. On Fig. 3(e), we compare [25] it to $\eta_{\text{eff}}(d)$ obtained from shear data. It appears that $\tilde{\eta}_{\text{eff}}$, which stays close to the bulk value down to three-layer-thick films, is about 2 orders of magnitude lower than η_{eff} .

We propose the following explanation to this apparent paradox. Shear experiments are a straightforward way to measure η_{eff} , in contrast to squeeze-out experiments requiring modeling of the front dynamics to infer a viscosity. Therefore, we consider that the reliable results for $\eta_{\text{eff}}(d)$ are those from shear rheology. We are then left with the observation of squeeze-out fronts which, given the $\eta_{\text{eff}}(d)$ obtained in shear, travel much faster than expected from

the drag mechanism assumed in the BM picture. This suggests that, in contrast to what BM and we assumed in previous works [9,17], the front dynamics is not controlled by the coherent sliding of adjacent incompressible molecular layers ahead of the front. Indeed, another piece of information emerges from the force-distance profile of Fig. 1: between two steps, the film thickness is observed to decrease by about 3 Å as the force is increased. Such a thickness variation is reversible upon load reduction. This shows that layered OMCTS films are substantially compressible, hence contain a non-negligible amount of free volume, which is consistent with the fact that confined films do not reach jamming. This certainly facilitates local rearrangements, and it is likely that during propagation of a front, molecules in the region ahead of it permeate between layers in order to accommodate for density variations. The apparent low resistance to front propagation suggests that permeation, rather than large scale coherent sliding of layers, controls mass transport ahead of the fronts. Related to this, it should also be noted that the boundary between n and $n - 1$ is a “defect” where the thickness is not an integer number of monolayers, and that transport properties in this defective region will contribute to front dynamics. A recent AFM study [21] concluded that OMCTS confined in such noninteger gaps exhibited a quasibulk viscosity, which may be connected to the present observations.

In summary, we have probed the rheology of a simple fluid under molecular confinement, and conclude that its behavior is akin to that of a sheared supercooled liquid close above the glass transition. This shows, as suggested by recent experiments on colloids [11], that confinement can be used as an alternative route to finely control the approach to jamming. Our results now raise two important questions. (i) We observe a liquidlike behavior down to the thinnest film investigated, which brings up the issue of how to cross the jamming transition under confinement. Two routes can be envisaged. It can be done by varying the corrugation of the walls, as shown in friction experiments [26] or in numerical simulations [12,27], or, as mentioned above, by changing the orientation between the crystalline lattices of the confining surfaces. (ii) We find that six-layer-thick films already exhibit a viscosity 2 orders of magnitude larger than the bulk value. This raises the question of the scale below which nonbulk behavior appears, and how it compares to the range of surface forces.

We thank A. N. Morozov for fruitful discussion and C. Caroli for critical reading of the manuscript.

*bureau@insp.jussieu.fr

- [1] M.D. Demetriou *et al.*, *Phys. Rev. Lett.* **97**, 065502 (2006), and references therein. J.H. Simmons *et al.*, *J. Non-Cryst. Solids* **105**, 313 (1988).
- [2] A. Furukawa *et al.*, *Phys. Rev. Lett.* **102**, 016001 (2009); V. Lubchenko, *Proc. Natl. Acad. Sci. U.S.A.* **106**, 11506 (2009); F. Varnik and O. Henrich, *Phys. Rev. B* **73**, 174209 (2006); L. Berthier and J.L. Barrat, *J. Chem. Phys.* **116**, 6228 (2002); R. Yamamoto and A. Onuki, *Phys. Rev. E* **58**, 3515 (1998); P. Sollich, *Phys. Rev. E* **58**, 738 (1998); V. Koblelev and K. S. Schweizer, *Phys. Rev. E* **71**, 021401 (2005).
- [3] M. Fuchs and M.E. Cates, *Phys. Rev. Lett.* **89**, 248304 (2002); K. Miyazaki and D.R. Reichman, *Phys. Rev. E* **66**, 050501(R) (2002).
- [4] M. Siebenburger *et al.*, *J. Rheol.* **53**, 707 (2009).
- [5] M.L. Gee *et al.*, *J. Chem. Phys.* **93**, 1895 (1990).
- [6] A.L. Demirel and S. Granick, *Phys. Rev. Lett.* **77**, 2261 (1996).
- [7] E. Kumacheva and J. Klein, *J. Chem. Phys.* **108**, 7010 (1998).
- [8] H. Yoshizawa and J.N. Israelachvili, *J. Phys. Chem.* **97**, 11 300 (1993).
- [9] T. Becker and F. Mugele, *Phys. Rev. Lett.* **91**, 166104 (2003). *Mol. Simul.* **31**, 489 (2005).
- [10] B.N.J. Persson and E. Tosatti, *Phys. Rev. B* **50**, 5590 (1994).
- [11] C.R. Nugent *et al.*, *Phys. Rev. Lett.* **99**, 025702 (2007).
- [12] B.N.J. Persson, *Sliding Friction*, Nanoscience and Technology Series (Springer, New York, 2000).
- [13] J.C.T. Eijkel and A. van den Berg, *Microfluid. Nanofluid.* **1**, 249 (2005), and references therein.
- [14] L. Bureau, *Rev. Sci. Instrum.* **78**, 065110 (2007).
- [15] J.N. Israelachvili, *J. Colloid Interface Sci.* **44**, 259 (1973).
- [16] M. Heuberger, *Rev. Sci. Instrum.* **72**, 1700 (2001).
- [17] L. Bureau and A. Arvengas, *Phys. Rev. E* **78**, 061501 (2008).
- [18] P. Frantz and M. Salmeron, *Tribol. Lett.* **5**, 151 (1998).
- [19] H.K. Christenson *et al.*, *J. Chem. Phys.* **87**, 1834 (1987).
- [20] $\sigma(\dot{\gamma})$ have been measured under a pressure p going from 1.5 MPa ($n = 6$) to 7.5 MPa ($n = 2$). We have checked that σ depends weakly on p at constant thickness. Its increase thus cannot be ascribed to an increase in p , and is due to geometrical confinement.
- [21] A. Maali *et al.*, *Phys. Rev. Lett.* **96**, 086105 (2006).
- [22] S.J. O’Shea and M.E. Welland, *Langmuir* **14**, 4186 (1998); G.B. Kaggwa *et al.*, *Appl. Phys. Lett.* **93**, 011909 (2008).
- [23] J.N. Israelachvili *et al.*, *Langmuir* **22**, 2397 (2006).
- [24] H. Yoshizawa and J.N. Israelachvili, *Thin Solid Films* **246**, 71 (1994); Y. Zhu and S. Granick, *Phys. Rev. Lett.* **87**, 096104 (2001).
- [25] We compare, for each d , $\tilde{\eta}_{\text{eff}}$ with η_{eff} measured at a shear velocity V equal to the average front velocity.
- [26] L. Bureau, and C. Caroli, and T. Baumberger, *Phys. Rev. Lett.* **97**, 225501 (2006).
- [27] K.G. Ayappa and R.K. Mishra, *J. Phys. Chem. B* **111**, 14 299 (2007).